RSC Advances

PAPER

View Article Online
View Journal | View Issue

Cite this: *RSC Adv.*, 2026, **16**, 3868

Bioactive metabolites from cultures of the entomopathogenic fungus *Pleurocordyceps ophiocordycipiticola* TBRC-BCC 9612

Siriporn Saepua,[a] Karoon Sadorn,[b] Jittra Kornsakulkarn,[a] Patchanee Auncharoen,[a] Suchada Mongkolsamrit,[a] Donnaya Thanakitpipattana[a] and Chawanee Thongpanchang *[a]

Pleurocordyceps ophiocordycipiticola TBRC-BCC 9612, an entomopathogenic fungus collected from Khao Yai National Park, Thailand, was investigated for its secondary metabolites. Large-scale fermentation, followed by multistep chromatographic separation, resulted in the isolation of seven new compounds, including an ergot-type alkaloid (dihydroergopleurine, **2**), three tetramic acid derivatives (pleurocordines A–C, **4–6**), two acyclic terpenoids (**7** and **8**), and a dihydroisobenzofuran derivative (**9**), along with twelve known compounds. The structures of the new compounds were elucidated based on spectroscopic analyses, including 1D and 2D NMR, HRMS, and ECD data. Selected compounds were evaluated for antimalarial activity against *Plasmodium falciparum* K1, antibacterial activity against *Bacillus cereus*, *Staphylococcus aureus*, and *Acinetobacter baumannii*, antifungal activity against phytopathogens (*Alternaria brassicicola* and *Colletotrichum acutatum*), as well as cytotoxicity toward cancerous (MCF-7, NCI-H187) and non-cancerous (Vero) cells. Among them, ergot alkaloids dihydroergosine (**1**) and dihydroergopleurine (**2**) showed antimalarial and cytotoxic activities, while pleurocordine C (**6**) demonstrated antibacterial and weak cytotoxic effects. 14-*Nor*-epicoccarine A (**3**) and pleurocordine A (**4**) exhibited moderate antifungal activity, and the known akanthomycin showed broad-spectrum bioactivity but lacked selectivity between cancerous and normal cells. These findings expand the chemical diversity known from *P. ophiocordycipiticola* and highlight several compounds with promising biological profiles for further pharmacological study.

Received 19th December 2025
Accepted 8th January 2026

DOI: 10.1039/d5ra09809b

rsc.li/rsc-advances

Introduction

Fungi represent a prolific source of bioactive secondary metabolites, many of which have found application in medicine, agriculture, and biotechnology.[1,2] Their diverse biosynthetic capacities are driven by ecological pressures and evolutionary adaptations, making them a valuable reservoir for novel chemical entities.[3,4] Among the rich diversity of fungi, entomopathogenic species within the order Hypocreales have been recognized for their capacity to produce structurally unique and pharmacologically active metabolites, including antimicrobial, antiviral, antitumor, and immunomodulatory effects.[5–7] Notably, members of the family Ophiocordycipitaceae, including genera such as *Ophiocordyceps* and *Tolypocladium*, are well known for their ability to produce key bioactive compounds such as cordycepin and cyclosporine.[8,9]

Pleurocordyceps ophiocordycipiticola is a recently described entomopathogenic fungus residing in the family Ophiocordycipitaceae.[10] Although its taxonomy and phylogenetics have been studied in recent years, knowledge about its chemical constituents remains limited. In general, species in the genus *Pleurocordyceps* have shown significant potential for the production of diverse bioactive compounds. Prior investigations revealed that *Pleurocordyceps nipponicus* and *P. phaothaiensis* produce natural antioxidants, antibacterial agents, anti-inflammatory molecules, and compounds with antitumorigenic and antimicrobial properties.[11–13] Moreover, Gokhale *et al.*[14] reported that metabolites derived from *P. sinensis* exhibit potent antibacterial effects, further highlighting the pharmacological potential of this genus.

In the course of our ongoing research on the bioactive potential of insect-associated fungi, we examined the crude extract of *Pleurocordyceps ophiocordycipiticola* TBRC-BCC 9612 cultured under laboratory conditions. A crude ethyl acetate extract of the fungal demonstrated significant cytotoxic activity against the human breast cancer cell line MCF-7, with an IC_{50}

[a]*National Center for Genetic Engineering and Biotechnology (BIOTEC), National Science and Technology Development Agency (NSTDA), 111 Thailand Science Park, Phahonyothin Road, Khlong Nueng, Khlong Luang, Pathum Thani 12120, Thailand. E-mail: chawanee@biotec.or.th*

[b]*Department of Chemistry, Faculty of Science, King Mongkut's Institute of Technology Ladkrabang, Chalongkrung Road, Ladkrabang, Bangkok 10520, Thailand*

value of 5.91 μg mL^{-1}, suggesting promising antitumor potential. Considering the bioactivities reported in related *Pleurocordyceps* species, together with the cytotoxic properties observed in this study, *P. ophiocordycipiticola* TBRC-BCC 9612 is a promising candidate for further chemical investigation to uncover its bioactive compounds. Herein, we report the isolation and characterization of the chemical constituents of this fungus, along with an evaluation of their biological activities.

Results and discussion

The cultured biomass of *P. ophiocordycipiticola* TBRC-BCC 9612 was extracted with ethyl acetate to yield a dark brown crude extract. Subsequent chromatographic purification led to the isolation of seven new compounds (**2** and **4–9**, Fig. 1), along with twelve previously reported compounds.

Dihydroergosine (**1**) was derived as a pale-yellow solid with a molecular formula determined as $C_{30}H_{39}N_5O_5$ from the protonated molecular ion observed in the high-resolution electrospray ionization mass spectrometry (HRESIMS) analysis. This compound was first isolated from the sclerotia of *Sphacelia sorghi* in 1968 [15] and has been synthetically derived *via* hydrogenation of ergosine since 1943.[16] However, to the best of our knowledge, no detailed NMR spectroscopic data for this compound has been reported in the literature to date. The ^1H, ^{13}C, and HSQC NMR spectra of **1** revealed the presence of three exchangeable protons (δ_H 11.58, 10.51, and 7.83), four aromatic protons, six methine, seven methylene and four methyl groups (Table 1). In addition, one oxygenated carbon (δ_C 104.4) and three carbonyl carbons (δ_C 166.6, 167.7, and 177.7) were observed. The lysergic moiety of the molecule was established based on interpretation of ^1H–^1H COSY and HMBC correlations. Analysis of the ^1H–^1H COSY spectrum indicated the proton–proton connectivity of NH-1/H-2, H-4/H-5/H-10/H-9/H-8/H-7, and H-12/H-13/H-14 spin systems. Key HMBC correlations (Fig. 2) from H-1 to C-3/C-16, H-2 to C-3/C-4/C-15/C-16, H-4 to C-2/C-3/C-10/C-16, H-5 to C-17, H-7 to C-5/C-9/C-17/C-18, H-8 to C-18, H-9 to C-5/C-11/C-18, H-10 to C-5/C-11/C-12, H-12 to C-10/C-14/C-16, H-13 to C-11/C-15, H-14 to C-12/C-16, and H-17 to C-5/C-7, enabled the assembly of lysergic acid skeleton. Furthermore, long-range HMBC correlations from H-19 to C-18/C-2′/C-3′/C-13′, along with the correlation from H-13′ to C-2′/C-3′, suggested the presence of an alanine residue linked to the lysergic acid moiety *via* an amide bond. The connectivity of H-5′/H-14′/H-15′/H-16′/H-17′, as revealed by ^1H–^1H COSY correlations, along with key HMBC correlations from H-5′ to C-3′/C-6′/C-12′, H-14′ to C-6′/C-16′/C-17′, H-15′ to C-16′/C17′, H-16′ and H-17′ to C-14′/C-15′, established the presence of a leucine residue. The final amino acid was identified as proline, based on ^1H–^1H COSY correlations among H-8′/H-9′/H-10′ and H-11′, as well as key HMBC cross-peaks from H-8′ to C-11′ and from H-11′ to C-12′. Extensive research on ergot alkaloid chemistry conducted over several decades has established that the absolute configuration at C-5 of all naturally occurring ergopeptines is *R*, consistent with their biosynthetic origin from L-tryptophan.[17] In addition, since only L-amino acids are

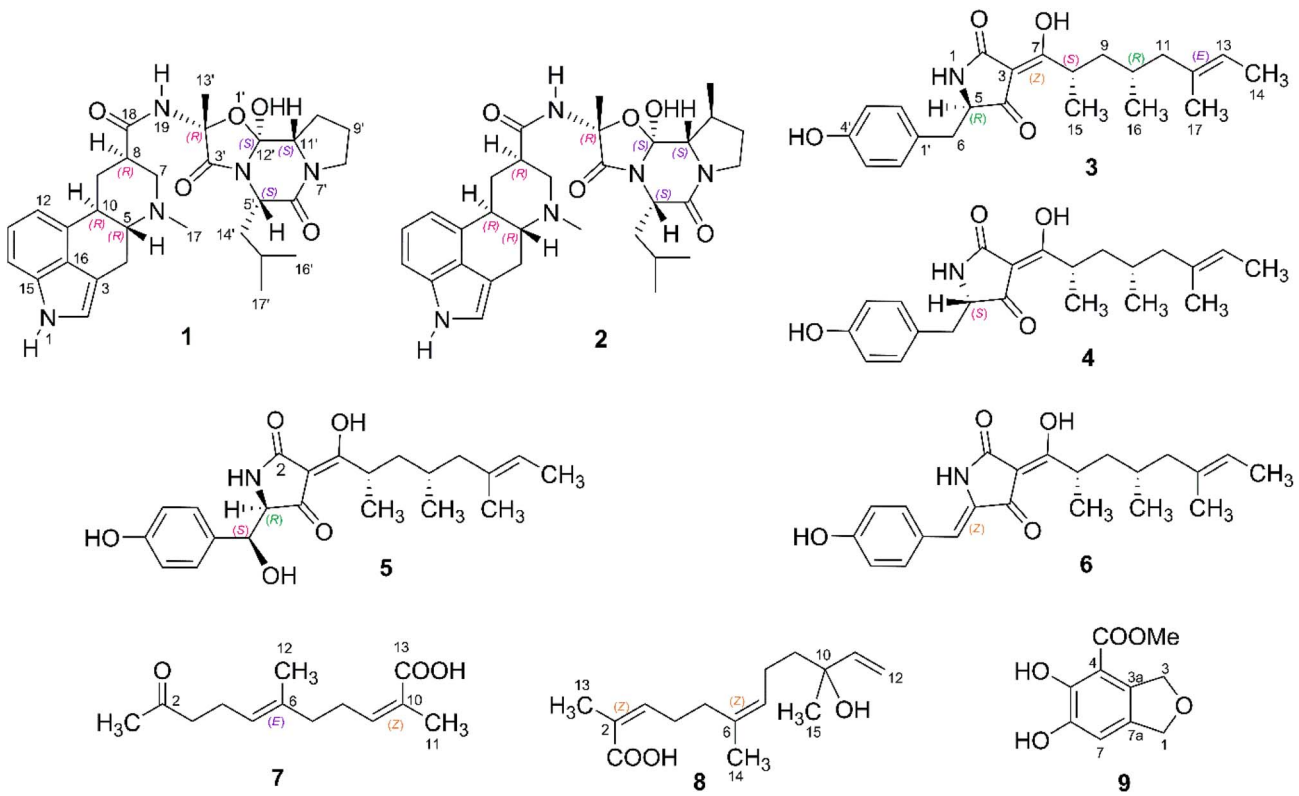

Fig. 1 Structure of compounds **1–9**.

Table 1 NMR spectroscopic data for compounds **1** and **2** in pyridine-d_5 (500 MHz for ^{1}H and 125 MHz for ^{13}C)

	1		**2**	
Position	δ_C	δ_H mult. (J in Hz)	δ_C	δ_H mult. (J in Hz)
2	119.6, CH	7.18 s	119.5, CH	7.17 s
3	111.8, C	—	111.8, C	—
4	27.8, CH_2	(a) 3.36 dd (3.7, 14.5) (b) 2.67 m	27.9, CH_2	(a) 3.35 dd (3.9, 14.6) (b) 2.66 m
5	67.8, CH	2.16 m	67.8, CH	2.15 m
7	60.2, CH_2	(a) 3.15 d (9.7) (b) 2.41 d (9.7)	60.2, CH_2	(a) 3.11 d (10.2) (b) 2.40 m
8	43.9, CH	3.16 m	43.9, CH	3.12 m
9	31.8, CH_2	(a) 2.89 m (b) 1.88 m	31.8, CH_2	(a) 2.87 m (b) 1.86 m
10	40.9, CH	2.90 m	41.0, CH	2.88 m
11	133.4, C	—	133.4, C	—
12	113.5, CH	6.79 d (7.1)	113.5, CH	6.79 d (7.0)
13	123.5, CH	7.22 dd (7.1, 8.1)	123.5, CH	7.23 dd (7.0, 8.1)
14	109.9, CH	7.38 d (8.1)	109.9, CH	7.38 d (8.1)
15	135.1, C	—	135.1, C	—
16	127.5, C	—	127.5, C	—
17	43.4, CH_3	2.28 s	43.4, CH_3	2.27 s
18	177.7, C	—	177.7, C	—
2′	87.4, C	—	87.4, C	—
3′	167.7, C	—	167.7, C	—
5′	54.3, CH	4.88 t (6.6)	54.2, CH	4.89 t (6.7)
6′	166.6, C	—	166.5, C	—
8′	46.9, CH_2	(a) 3.73 t (9.6) (b) 3.61 t (9.6)	46.3, CH_2	3.68 m
9′	22.8, CH_2	(a) 1.65 m (b) 1.84 m	31.5, CH_2	(a) 1.92 m (b) 1.37 m
10′	27.4, CH_2	(a) 2.13 m (b) 2.30 m	36.0, CH	2.68 m
11′	66.2, CH	3.76 dd (5.9, 10.3)	71.6, CH	3.29 d (10.0)
12′	104.4, C	—	104.6, C	—
13′	25.1, CH_3	1.98 s	25.0, CH_3	1.98 s
14′	44.7, CH_2	(a) 2.40 m (b) 2.35 dd (7.7, 14.6)	44.7, CH_2	(a) 2.43 m (b) 2.35 m
15′	25.8, CH	2.63 m	25.7, CH	2.63 m
16′	23.1, CH_3	1.15 d (6.4)	23.0, CH_3	1.16 d (6.3)
17′	23.5, CH_3	1.12 d (6.7)	23.6, CH_3	1.11 d (6.5)
18′	—	—	17.1, CH_3	1.25 d (6.3)
1-NH	—	11.58 s	—	11.58 s
19-NH	—	10.51 s	—	10.48 s
12′-OH	—	7.83 br s	—	7.94 br s

incorporated into the tricyclic peptide moiety,[18,19] the absolute configurations at C-2′, C-5′, C-11′, and C-12′ were proposed to be *R*, *S*, *S*, and *S*, respectively. A key cross-peak observed in the NOESY spectrum (Fig. 2) indicated a spatial correlation between H-8 and H-10, while no correlation was detected between H-5 and H-10. This suggests that H-8 and H-10 are located on the same face of the ring system, whereas H-5 resides on the opposite face. These observations support the assignment of 8*R* and 10*R* configurations. The specific rotation value of **1** ($[\alpha]_D^{27}$ +9.73, *c* 0.10) was consistent with those previously reported for both natural product ($[\alpha]_D^{20}$ +5.9, *c* 4.3)[15] and its synthetic counterpart ($[\alpha]_D^{20}$ +10.1, *c* 1.5),[16] further supporting the proposed stereochemistry.

Dihydroergopleurine (**2**) was obtained as a pale-brown solid. Its molecular formula was determined to be $C_{31}H_{41}N_5O_5$, which is 14 mass units higher than that of **1**, based on HRESIMS. The ^{1}H and ^{13}C NMR spectra of **2** closely resembled those of **1**, suggesting a similar structural framework. Detailed analysis of 2D NMR spectroscopic data revealed that **2** shares the same core structure as **1**, with the key difference being the presence of an additional methyl group at C-10′. The location of this methyl substituent was confirmed by its ^{1}H–^{1}H COSY correlation with H-10′ and HMBC correlations to C-9′/C-10′/C-11′. Furthermore, a NOESY correlation between the methyl protons and H-11′ supported the assignment of 10′*S* configuration. In addition, the electronic circular dichroism (ECD) spectrum of **2** was almost identical to that of **1** (Fig. 3), suggesting that both compounds possess the same absolute configurations at C-2′, C-5′, C-11′, and C-12′.

The HRESIMS data for compounds **3** and **4** gave the same molecular formula of $C_{22}H_{29}NO_4$. Their ^{1}H and ^{13}C NMR spectra recorded in acetone-d_6 were also highly similar (Table

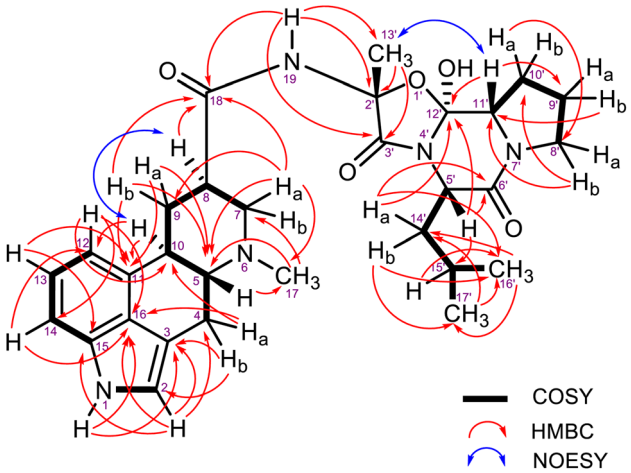

Fig. 2 Key COSY, HMBC and NOESY correlations of compound **1**.

2), indicating the presence of four methyl groups, three methylene units, four aromatic methines, four additional methine carbons (including one sp^2 carbon), and seven quaternary carbons, among which two are carbonyls and one is a carboxamide carbon. Analysis of 2D NMR spectroscopic data revealed that both compounds share a common structural framework closely related to epicoccarine A, as previously reported by Kemami Wangun *et al.*[20] This structure includes a *para*-hydroxyphenyl moiety originating from a tyrosine-derived unit and a substituted aliphatic side chain, both connected through a tetramic acid core. The structures of the aliphatic side chains attached to C-7 in compounds **3** and **4** differ from that of epicoccarine A. HMBC correlations from the methyl protons H-15 to C-7/C-8/C-9, H-16 to C-9/C-10/C-11, H-17 to C-11/C-12/C-13, and H-14 to C-12/C-13 indicated that the methyl groups at C-15, C-16, C-17, and C-14 are positioned at C-8, C-10, C-12, and C-13, respectively. Analysis of the NOESY spectra revealed spatial correlations between H-11 and H-13, H-14 and H-17, and H-16 and H-17, supporting the assignment of an *E* configuration for the $\Delta^{12,13}$ double bond (Fig. 4). The ^{13}C NMR chemical shifts observed for C-2 and C-4 of the tetramic acid cores in **3** and **4** were closely comparable to those reported for synthetic epicoccarine A and 5-*epi*-epicoccarine A, both of which possess a *Z* configuration at the $\Delta^{3,7}$ double bond.[21] Furthermore, comparison with the ^{13}C NMR chemical shifts of the *Z*- and *E*-isomers of F-14329 reported by Shang and co-workers[22] ($\delta_{C\text{-}2}$ 175.7 and $\delta_{C\text{-}4}$ 194.7 for the *Z*-isomer, and $\delta_{C\text{-}2}$ 169.2 and $\delta_{C\text{-}4}$ 201.2 for the *E*-isomer) strongly supported that compounds **3** and **4** possess $\Delta^{3,7}$ double bonds in the *Z*-enol tautomeric form.

However, compounds **3** and **4** exhibited opposite optical rotations, with **3** showing a negative value ($[\alpha]_D^{25}$ −116.9, *c* 0.09, MeOH) and **4** a positive value ($[\alpha]_D^{25}$ +77.8, *c* 0.10, MeOH). In addition, their ECD spectra displayed mirror-image Cotton effects (Fig. 5), further confirming that these two compounds are epimers at C-5. The absolute configurations at C-5 were assigned as *S* for compound **3** and *R* for compound **4**, based on comparison of their optical rotation values with those previously reported for epicoccarine A ($[\alpha]_D^{25}$ −161.8, *c* 0.15, MeOH) and 5-*epi*-epicoccarine A ($[\alpha]_D^{25}$ +97.5, *c* 0.15, MeOH).[21] The chemical structure of compound **3** is consistent with that of 14-*nor*-epicoccarine B previously isolated from *Penicillium aurantiacobrunneum*,[23] however, the stereochemical configuration at C-5 in that report was not unambiguously assigned. In this study, compound **4** was designated as pleurocordine A.

Compound **5** was obtained as a pale-yellow solid, and its molecular formula was determined to be $C_{22}H_{29}NO_5$, as established by the sodium-adduct ion peak at *m*/*z* 410.1937 $[M + Na]^+$ in the HRESIMS spectrum. This molecular weight is 16 amu

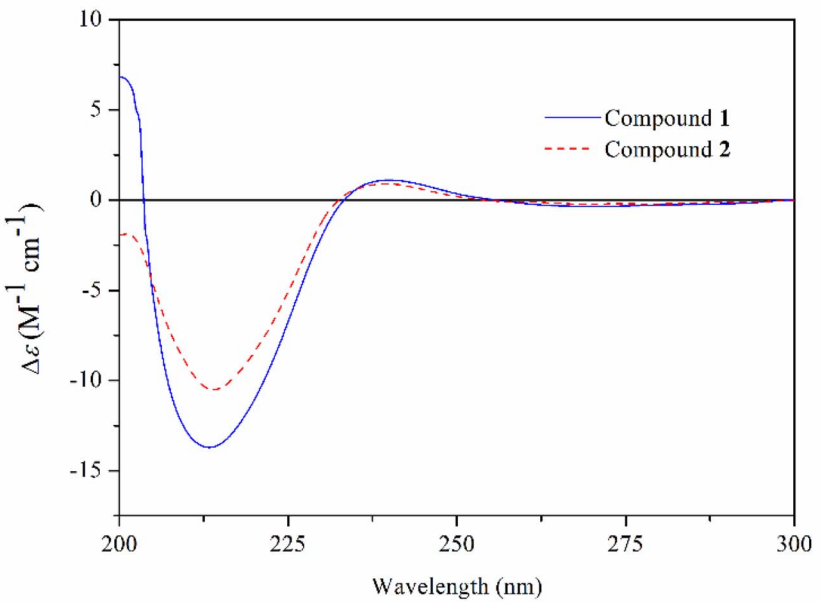

Fig. 3 ECD spectrum of compounds **1** and **2**.

Table 2 NMR spectroscopic data for compounds 3–6 (500 MHz for ^{1}H and 125 MHz for ^{13}C)

	3[a]		4[a]		5[a]		6[b]	
Position	δ_C	δ_H mult. (J in Hz)	δ_C	δ_H mult. (J in Hz)	δ_C	δ_H mult. (J in Hz)	δ_C	δ_H mult. (J in Hz)
2	176.7, C	—	176.3, C	—	177.2, C	—	—[c]	—
3	101.6, C	—	101.9, C	—	102.6, C	—	—[c]	—
4	195.2, C	—	195.3, C	—	194.2, C	—	181.0, C[d]	—
5	64.0, CH	4.09 br s	63.6, CH	4.10 br s	68.6, CH	4.03 br s	—[c]	—
6	37.3, CH_2	(a) 3.02 dd (4.0, 13.9) (b) 2.87 dd (5.7, 13.9)	36.9, CH_2	(a) 3.00 dd (3.8, 14.0) (b) 2.93 dd (4.9, 14.0)	72.6, CH	5.05 d (1.7)	110.0, CH	6.45 s
7	192.5, C	—	192.0, C	—	191.3, C	—	199.2, C[d]	—
8	34.4, CH	3.76 m	34.2, CH	3.77 m	34.2, CH	3.80 m	35.8, CH[d]	3.82 m
9	40.9, CH_2	(a) 1.75 m (b) 1.08 m	41.0, CH_2	(a) 1.71 m (b) 1.01 m	41.2, CH_2	(a) 1.77 m (b) 1.08 m	39.8, CH_2	(a) 1.71 m (b) 1.08 m
10	29.6, CH	1.52 m	29.3, CH	1.36 m	29.3, CH	1.55 m	28.4, CH	1.49 m
11	48.8, CH_2	(a) 1.92 dd (6.9, 12.8) (b) 1.78 dd (7.0, 12.8)	48.8, CH_2	(a) 1.88 m (b) 1.81 m	48.9, CH_2	(a) 1.92 m (b) 1.80 m	47.5, CH_2	(a) 1.89 dd (6.9, 13.3) (b) 1.75 m
12	135.0, C	—	135.2, C	—	135.2, C	—	134.0, C	—
13	120.5, CH	5.17 q (6.6)	120.5, CH	5.16 q (6.5)	120.4, CH	5.18 q (6.6)	119.4, CH	5.14 dq (1.1, 6.7)
14	13.4, CH_3	1.54 d (6.6)	13.4, CH_3	1.55 d (6.5)	13.4, CH_3	1.56 d (6.6)	13.2, CH_3	1.53 d (6.7)
15	18.7, CH_3	1.06 d (6.8)	18.5, CH_3	1.11 d (6.8)	18.7, CH_3	1.14 d (6.8)	18.1, CH_3	1.11 d (6.6)
16	20.0, CH_3	0.82 d (6.2)	20.4, CH_3	0.85 d (6.5)	20.1, CH_3	0.83 d (6.5)	19.6, CH_3	0.79 d (6.6)
17	15.4, CH_3	1.51 s	15.3, CH_3	1.45 s	15.5, CH_3	1.52 s	15.2, CH_3	1.48 s
1′	127.4, C	—	127.2, C	—	133.3, C	—	124.0, C	—
2′/6′	131.6, CH	7.02 d (8.0)	131.7, CH	7.00 d (8.1)	128.1, CH	7.26 d (8.3)	131.7, CH	7.52 d (8.4)
3′/5′	115.8, CH	6.71 d (8.0)	115.8, CH	6.69 d (8.1)	115.8, CH	6.80 d (8.3)	115.8, CH	6.79 d (8.4)
4′	157.1, C	—	157.1, C	—	157.5, C	—	158.2, C	—
4′-OH	—	8.25[e] br s	—	8.24[e] br s	—	—	—	9.92 br s
1-NH	—	7.82[e] br s	—	7.84[e] br s	—	—	—	—

[a] In acetone-d_6. [b] In DMSO-d_6. [c] Some carbon signals are too weak or broad to be observed in the ^{13}C NMR spectrum. [d] Assignments were supported by HSQC and HMBC spectra. [e] Exchangeable.

higher than those of compounds **3** and **4**, suggesting the presence of an additional hydroxyl group in **5**. The ^{1}H and ^{13}C NMR spectroscopic data (Table 2) of **5** closely resembled those of compounds **3** and **4**, with the notable difference being the appearance of a hydroxymethine resonance at δ_H 5.05 (δ_C 72.55), assignable to C-6. The HMBC spectrum of H-6 displayed correlations to aromatic carbons C-1′, C-2′, and C-6′, as well as to the carbonyl carbon at C-4, thereby confirming its position. The NOESY spectrum of **5** was largely consistent with those of compounds **3** and **4**, showing key correlations between H-6 and H-6′, H-8 and H-10, H-9 and H-11, H-15 and H-16, and H-16 and H-17, further supporting the structural similarity and relative configuration within this series. Comparison of the ^{1}H NMR chemical shifts and the small ^3J coupling constant between H-5 and H-6 ($J_{5,6}$ = 1.6 Hz) with those of chaunolidine A[22] indicated a *cis*-relationship between the two protons. Furthermore, the ECD spectrum of compound **5** displayed a negative Cotton effect at 213 nm ($\Delta\varepsilon$ −0.6) and positive Cotton effects at 229 nm ($\Delta\varepsilon$ +0.8), 249 nm ($\Delta\varepsilon$ +0.2) and 287 nm ($\Delta\varepsilon$ +1.5) (Fig. 6), consistent with the previously reported spectrum of chaunolidine A ($\Delta\varepsilon$ (nm) −3.7 (213), +6.5 (229), +1.3 (249), +3.3 (284)). In addition, compound **5** exhibited a positive optical rotation ($[\alpha]_D^{25}$ +43.0, *c* 0.12, MeOH), also in agreement with chaunolidine A ($[\alpha]_D^{22}$ +70.4, *c* 0.05, MeOH).[22] Taken together, these data suggested that compound **5** possesses the absolute configuration 5*R*,6*S*. Therefore, compound **5** was named pleurocordine B.

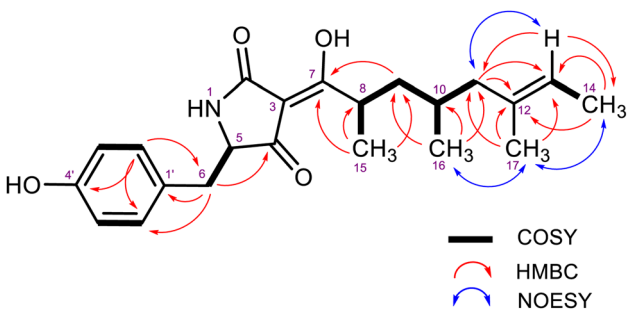

Fig. 4 Key COSY, HMBC and NOESY correlations of compounds **3** and **4**.

HRESIMS analysis of compound **6** revealed a molecular formula of $C_{22}H_{27}NO_4$, indicating that it is a dehydrated analogue of compound **5**. The ^{1}H and ^{13}C NMR spectra recorded in DMSO-d_6 showed signals attributable to four methyl groups, two methylene units, four aromatic methines, and four methine protons, including two sp^2-hybridized carbons. Additionally,

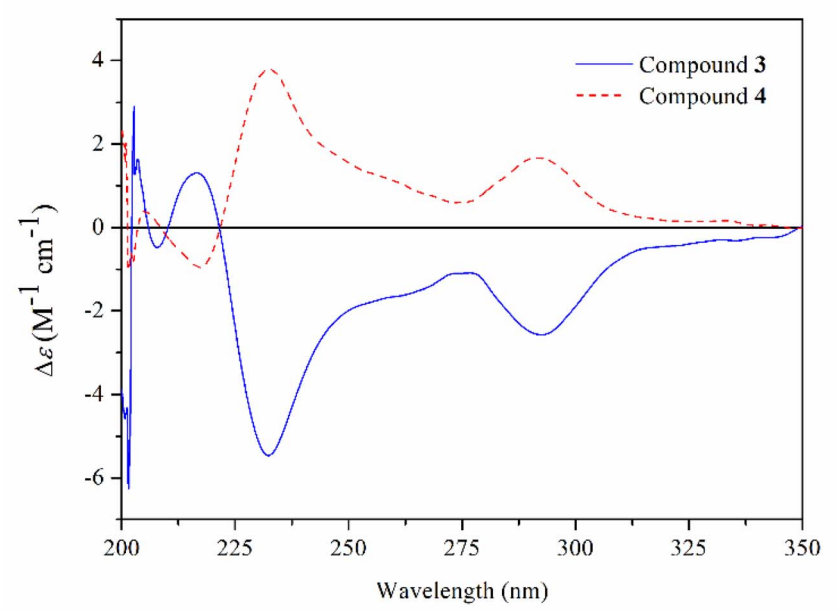

Fig. 5 ECD spectrum of compounds **3** and **4**.

eight quaternary carbons were observed, comprising two carbonyl carbons and one carboxamide carbon. Comparison with the NMR data of compound **5** confirmed the absence of a hydroxymethine carbon and the emergence of a sp^2 methine at C-6, resonating at δ_H 6.45 and δ_C 110.0. This new signal exhibited HMBC correlations to the carbonyl carbon at C-4 and the aromatic carbons at C-2′ and C-6′, establishing its position within the framework. The NOESY spectrum recorded in acetone d_6 showed key spatial correlations between H-2′/H-6′ and the amide NH proton of the tetramic acid ring, supporting the assignment of a *Z*-configuration for the $\Delta^{5,6}$ double bond. Accordingly, compound **6** was named pleurocordine C.

Considering that the structures of compounds **3–6** closely resemble those of known tetramic acid derivatives, their biosynthesis is likely to follow a similar pathway. A plausible biosynthetic route for these compounds can be proposed based on previously reported pathways for related natural products such as epicoccarine A, epipyridone, and tenellin.[20,24] The biosynthesis is expected to be mediated by a hybrid polyketide synthase–nonribosomal peptide synthetase (PKS–NRPS)

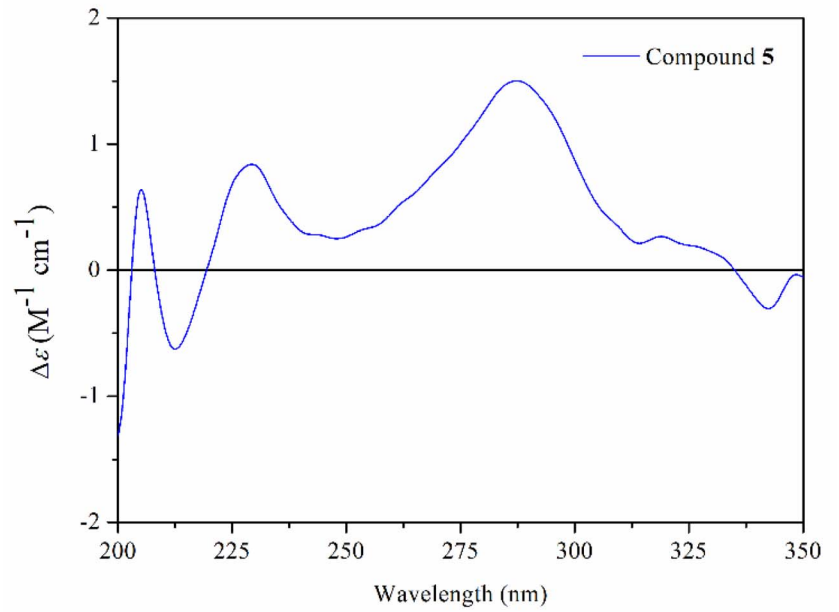

Fig. 6 ECD spectrum of compound **5**.

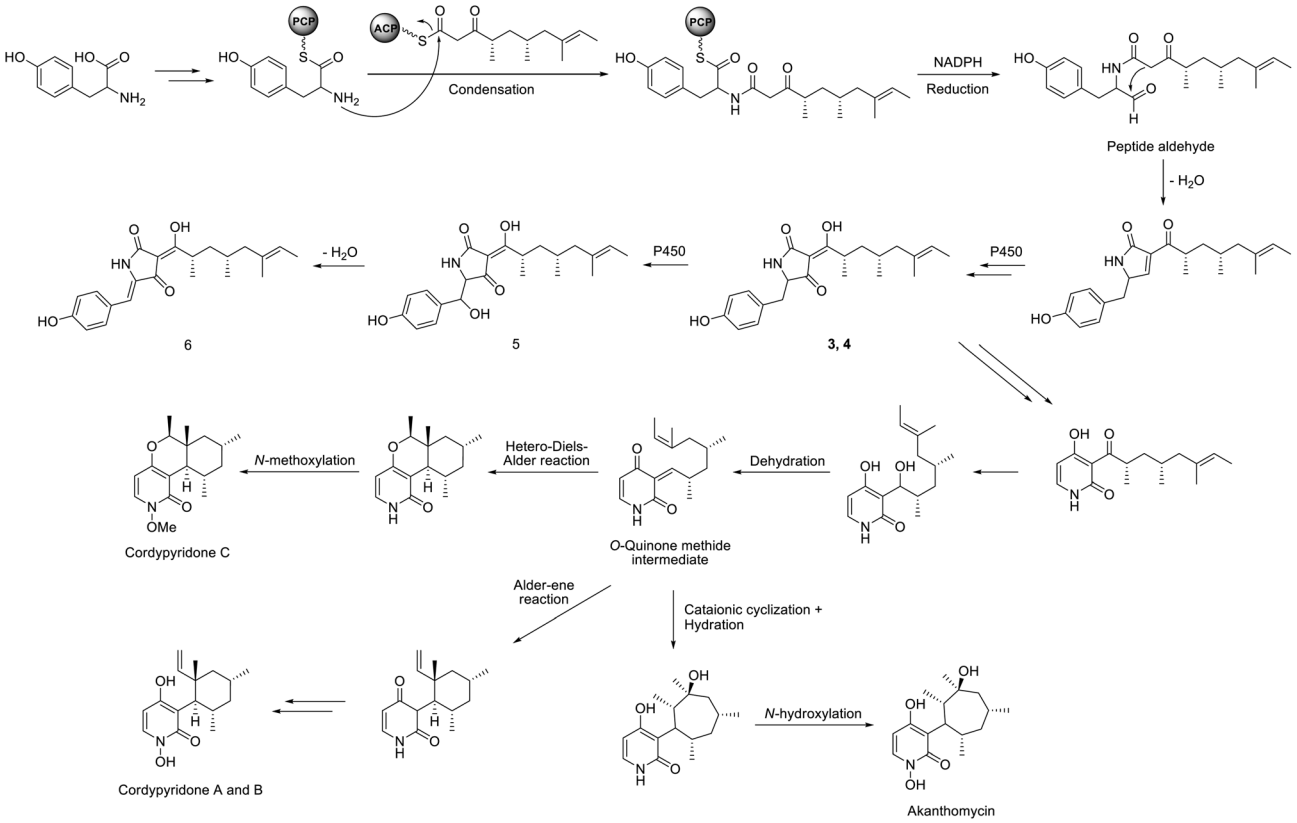

Fig. 7 Plausible biosynthetic pathway for compounds **3–6**, cordypyridones A–C and akanthomycin.

system, in which a polyketide chain is linked to the amino acid tyrosine *via* thioester condensation. Reductive cleavage of the thioester intermediate, followed by intramolecular cyclization and oxidations, furnishes the pyrrolidinone core structures represented by compounds **3** and **4**. Subsequent oxidative hydroxylation of either **3** or **4** at the C-6 position yields the hydroxy-containing compound **5**. Dehydration of **5** then affords the $\Delta^{5,6}$-unsaturated derivative **6**, completing a logical biosynthetic sequence that links these structurally related metabolites (Fig. 7).

Compounds **3** and **4** may serve as biosynthetic precursors to downstream pyrrolidinone-derived metabolites, as previously proposed by Ohashi *et al.*[25] These compounds can undergo enzymatic reduction followed by dehydration to generate an *ortho*-quinone methine intermediate.[26] This reactive intermediate is proposed to participate in divergent cyclization reactions depending on the reaction conditions or enzyme partners: a hetero-Diels–Alder reaction produces cordypyridone C, while an Alder–ene reaction results in the formation of cordypyridones A and B. Alternatively, cationic cyclization of the same intermediate can lead to the formation of akanthomycin (Fig. 7).

Based on this unified biosynthetic hypothesis, these compounds are inferred to share identical stereochemistry at C-8 and C-10, as they are co-metabolites derived from a common biosynthetic intermediate within the same pathway.

Compound **7** was isolated as a pale-yellow oil. Its molecular formula was determined to be $C_{13}H_{20}O_3$ based on positive HRESIMS, which exhibited a $[M + Na]^+$ ion at *m*/*z* 247.1306 (calcd for $C_{13}H_{20}O_3Na^+$: 247.1305). The IR spectrum displayed absorption bands at 3429, 1708, and 1644 cm^{-1}, corresponding to the stretching vibrations of hydroxyl, conjugated carboxylic acid carbonyl, and ketone functional groups, respectively. The ^1H and ^{13}C NMR spectroscopic data of compound **7** were nearly identical to those reported for 10-carboxy-6,10-dimethyl-5*E*,9*E*-undecadien-2-one, a known biotransformation product of geranylacetone.[27] However, detailed analysis of 2D NMR spectra revealed one structural difference, *i.e.* the configuration of the C-9/C-10 double bond. The ^1H–^1H COSY spectrum provided two key spin systems extending from H-3 to H-5 and from H-7 to H-9. The HMBC spectrum exhibited correlations from H-1 to C-2, H-3 to C-2/C-5, H-4 to C-2/C-6, H-5 to C-7/C-12, H-7 to C-5/C-6/C-9/C-12, H-8 to C-6/C-10, H-9 to C-7/C-10/C-11/C-13, and H-12 to C-5/C-6/C-7. In the NOESY spectrum, cross-peaks between H-4 and H-12, H-7 and H-5, and H-9 and H-11 supported the assignment of 5*E* and 9*Z* configurations for the two double bonds. Accordingly, compound **7** was identified as 10-carboxy-6,10-dimethyl-5*E*,9*Z*-undecadien-2-one.

Compound **8** was obtained as a pale-yellow oil. Its molecular formula was determined to be $C_{15}H_{24}O_3$ based on HRESIMS. Comparison of the ^1H and ^{13}C NMR spectroscopic data of **8** with those of 12-carboxylic acid derivative of *cis*-nerolidol, a known microbial oxidation product of *cis*-nerolidol,[28] suggested that both compounds share the same sesquiterpenoid core structure. This structural similarity was further confirmed by detailed analysis of 2D NMR spectroscopic data. Interpretation

of the ^{1}H–^{1}H COSY spectrum allowed the assignment of three partial spin systems: H-3/H-4/H-5, H-7/H-8/H-9, and H-11/H-12. Key HMBC correlations from H-3 to C-1/C-2/C-5/C-13, H-4 to C-2/C-6, H-5 to C-3/C-7/C-14, H-7 to C-5/C-6/C-9/C-14, H-8 to C-6/C-10, H-9 to C-7/C-10/C-11/C-15, H-11 to C-9/C-10/C-15, and H-12 to C-10 established the planar structure corresponding to nerolidol-12-carboxylic acid. Furthermore, NOESY correlations from H-3 to H-13, as well as between H-7 and H-14, supported the assignment of *Z* configurations at both the C-2/C-3 and C-6/C-7 double bonds. These stereochemical features differ from those previously reported for other 12-carboxylic acid derivatives of nerolidol, such as 2*E*,6*E* and 2*E*,6*Z* isomers.[28] Compound **8** was therefore identified as 10-hydroxy-2,6,10-trimethyl-2*Z*,6*Z*,11-dodecatrienoic acid, *i.e.* all-*cis*-nerolidol-12-carboxylic acid.

Compound **9** was derived as a pale-brown solid. The molecular formula was established to be $C_{10}H_{10}O_5$, based on the sodium-adduct molecular ion peak observed at *m*/*z* 233.0421 $[M + Na]^+$ in the HRESIMS spectrum. The ^{1}H and ^{13}C NMR spectra revealed characteristic signals for two exchangeable hydroxyl protons (δ_H 10.43 and 9.51), one aromatic proton, two oxygenated methylene groups, and one methyl group. In addition, the data also showed one carbonyl carbon and five quaternary aromatic carbons, two of which were substituted with oxygen atoms. The HMBC correlations from H-1 to C-3a/C-7a, H-3 to C-1/C-3a/C-7a, and H-7 to C-1/C-3a/C-5/C-6/C-7a enabled the construction of a 1,3-dihydrobenzofuran skeleton. The position of the methyl carboxylate group and two hydroxyl substituents at C-4 (δ_C 107.8), C-5 (δ_C 149.0), and C-6 (δ_C 145.7), respectively, were assigned based on the HMBC correlation between the methoxy protons and the ester carbonyl carbon, along with the characteristic ^{13}C chemical shifts of the oxygenated aromatic carbons. Therefore, compound **9** was identified as methyl-5,6-dihydroxy-1,3-dihydroisobenzofuran-4-carboxylate.

The structures of the known compounds were dereplicated from HRESIMS and NMR (^{1}H and ^{13}C) spectroscopic data. The known compounds were identified as akanthomycin,[29] cordypyridones A-C,[30] cordytropolone,[31] stipitalide,[32] 4-hydroxy-3,6-dimethyl-2*H*-pyran-2-one,[33] indole-2-carboxylic acid, 3-methyl-orcinaldehyde,[34] and *trans*–*trans*-farnesol.[35]

The biological activities of nine compounds isolated from the cultures of *Pleurocordyceps ophiocordycipititicola* TBRC-BCC 9612, including compounds **1–8** and the known antibiotic akanthomycin, were evaluated for antimalarial, antibacterial, antifungal, and cytotoxic effects (Table 3).

Among the tested compounds, akanthomycin exhibited the strongest antiplasmodial activity against *Plasmodium falciparum* K1 (IC_{50} = 2.00 μM). The ergot alkaloids **1** and **2** showed moderate activity, with IC_{50} values of 5.82 and 4.83 μM, respectively, suggesting this scaffold may be relevant for further antimalarial development. The remaining compounds, including those in a series of tetramic acid derivatives (**3–6**), and sesquiterpenoids (**7** and **8**), exhibited no antimalarial activity (IC_{50} > 25 μM).

Only a few compounds exhibited notable antibacterial activity. Compound **1** displayed selective activity against *Bacillus cereus* (MIC = 0.28 μg mL^{-1}) but was inactive against other tested strains. In contrast, compound **6**, a member of tetramic acid derivatives, showed activity not only against *B. cereus* but also against *Staphylococcus aureus* (MIC = 3.13 μg mL^{-1} for both strains). Akanthomycin also inhibited both *B. cereus* and *S.*

Table 3 Biological activities of compounds **1–8** and akanthomycin from cultures of *Pleurocordyceps ophiocordycipititicola* TBRC-BCC 9612

Compounds	Antimalarial *P. falciparum*, K1 (IC_{50}, μM)	Anti-bacterial (MIC, μg mL^{-1})			Anti-phytopathogenic fungal (MIC, μg mL^{-1})		Cytotoxicity (IC_{50}, μM)		
		B. cereus	*A. baumannii*	*S. aureus*	*C. acutatum*	*A. brassicicola*	NCI-H187	MCF-7	Vero
1	5.82	0.28	>50	>50	>50	>50	39.28	89.98	81.80
2	4.83	>50	>50	>50	>50	>50	58.76	62.04	54.60
3	>26.92	NT	>50	25.00	12.50	25.00	NT	NT	45.66
4	>26.92	NT	>50	12.50	12.50	25.00	NT	NT	43.29
5	>25.81	NT	>50	25.00	50.00	50.00	NT	NT	44.83
6	>27.07	3.13	>50	3.13	>50	>50	110.8	>135.3	89.16
7	>44.58	>50	>50	>50	>50	>50	>222.9	>222.9	>222.9
8	>39.63	>50	>50	>50	>50	>50	>198.1	>198.1	>198.1
Akanthomycin	2.00	6.25	>50	6.25	>50	>50	2.22	4.06	1.59
Dihydroartemisinin[a]	0.002–0.003	—	—	—	—	—	—	—	—
Chloroquine diphosphate[a]	0.300–0.617	—	—	—	—	—	—	—	—
Rifampicin[b]	—	0.195–0.391	3.13	0.078–1.56	—	—	—	—	—
Vancomycin[b]	—	3.13	—	1.00–2.00	—	—	—	—	—
Amphotericin B[c]	—	—	—	—	1.56–6.25	0.781–6.25	—	—	—
Doxorubicin[d]	—	—	—	—	—	—	0.105	18.25	—
Ellipticine[d]	—	—	—	—	—	—	8.24	—	2.49–7.39
Tamoxifen[d]	—	—	—	—	—	—	—	46.70	—

[a] Positive control for antimalarial assay. [b] Positive control for antibacterial assay. [c] Positive control for antifungal assay. [d] Positive control for cytotoxicity assay. NT = not tested (due to a shortage of samples).

aureus with equal MIC values (6.25 μg mL^{-1}). No compounds showed significant activity against *Acinetobacter baumannii*. These results suggest that structural features such as the benzylidene-substituted pyrrolidinedione core in compound **6** may contribute to broader antibacterial activity, particularly against Gram-positive pathogens.

Antifungal activity was observed only in specific members of the tetramic acid derivatives. Compounds **3** and **4**, stereoisomers at C-5 of the pyrrolidine ring, both exhibited moderate activity against the phytopathogenic fungi *Colletotrichum acutatum* and *Alternaria brassicicola* (MIC = 12.5 and 25.0 μg mL^{-1}, respectively). In contrast, the hydroxylated derivative **5** and its dehydration product **6** were inactive against both fungal strains (MIC ≥ 50 μg mL^{-1}), suggesting that hydroxylation or conjugation at the benzyl moiety may reduce antifungal activity. Akanthomycin showed no activity against either fungus, in line with its primary known antibacterial profile. These findings indicate that the 5-benzylpyrrolidine-2,4-dione framework can confer selective antifungal activity independent of stereochemical conformation.

Among the ergot-type alkaloids, **1** exhibited cytotoxicity against NCI-H187 (IC_{50} = 39.28 μM), with selectivity over the non-cancerous Vero cells (IC_{50} = 81.80 μM). Its methylated analog **2** showed broader but less selective cytotoxicity toward both NCI-H187 and MCF-7 cancer lines (IC_{50} = 55.76 and 62.04 μM, respectively), and lower Vero cell toxicity (IC_{50} = 54.60 μM). In the pyrrolidinedione series, compound **6** was the only member tested against cancer lines and exhibited weak cytotoxicity (IC_{50} > 110 μM). Interestingly, compounds **3–5**, although not tested against cancer cell lines, demonstrated low toxicity against Vero cells (IC_{50} ~43–45 μM), indicating mild non-specific cytotoxicity. Akanthomycin stood out for its potent cytotoxicity across both cancerous and non-cancerous cell lines (IC_{50} = 1.59–4.06 μM), but its lack of selectivity limits its interest as a potential therapeutic agent.

The bioactivity profiles reveal two promising scaffolds. First, the ergot-type alkaloids (**1** and **2**) showed consistent moderate antimalarial and cytotoxic effects, suggesting the lysergic acid core as a valuable pharmacophore for further optimization. Second, the pyrrolidine-2,4-dione class demonstrates structural diversity in biological profiles. Compounds **3** and **4** were moderately antifungal, while **6**, bearing a benzylidene conjugation, displayed antibacterial and mild cytotoxic properties. Subtle modifications, such as hydroxylation in **5** or dehydration in **6**, markedly affected bioactivity, indicating a sensitive SAR within this class. In contrast, the sesquiterpenoids **7** and **8** were inactive in all assays, suggesting that additional functional groups or molecular complexity are required for significant biological effects.

Conclusions

This study explored the secondary metabolite profile of *P. ophiocordycipititicola* TBRC-BCC 9612 and led to the isolation of seven new compounds and twelve known metabolites. The isolated compounds exhibited diverse bioactivities across multiple targets. Notably, the ergot-type alkaloids (**1** and **2**) displayed moderate antimalarial and cytotoxic properties. The pyrrolidine-2,4-dione series (**3–6**) revealed substitution-dependent antifungal and antibacterial activity, demonstrating the structural sensitivity of this scaffold. Akanthomycin exhibited potent but non-selective antimicrobial and cytotoxic effects. These results provide valuable insights into the chemical and biological potential of *P. ophiocordycipititicola*, supporting its role as a promising source of structurally diverse and bioactive fungal metabolites.

Experimental

General experimental procedures

Melting points were determined using a Mettler MP90 melting point apparatus and are uncorrected. Optical rotations were measured with a JASCO P-1030 digital polarimeter. Electronic circular dichroism (ECD) spectra were recorded on a JASCO J-810 spectropolarimeter. UV and FT-IR spectra were obtained using an Analytik-Jena SPEKOL 1200 UV-vis spectrophotometer and a Bruker Alpha FT-IR spectrometer, respectively. NMR spectra were recorded on a Bruker Advance III 400 (400 MHz for ^{1}H and 100 MHz for ^{13}C) and Bruker Advance 500 (500 MHz for ^{1}H and 125 MHz for ^{13}C) spectrometers. Chemical shifts (δ) are reported in parts per million (ppm), with reference to residual solvent signals. High-resolution electrospray ionization mass spectrometry (HRESIMS) data were acquired using a Bruker micrOTOF mass spectrometer. Column chromatography was carried out on silica gel 60 (60–200 mesh, Merck). High-performance liquid chromatography (HPLC) was performed on a Dionex Ultimate 3000 system equipped with a binary pump, autosampler, and diode array detector (DAD), using reversed-phase columns under gradient or isocratic conditions as specified.

Fungal material

Pleurocordyceps sp. is an entomopathogenic fungus isolated from a hymenopteran ant collected from leaf litter in Khao Yai National Park, Thailand. The axenic culture was deposited in the BIOTEC Culture Collection (BCC), Thailand, under the accession number BCC 9612. Genomic DNA was extracted, and sequences of the internal transcribed spacer (ITS), large subunit ribosomal RNA gene (LSU rDNA), translation elongation factor 1-alpha (*TEF1*), and RNA polymerase II largest subunit (*RPB1*) were obtained following the protocol of Mongkolsamrit *et al.*[36] These sequences have been deposited in GenBank under accession numbers PX701911 (ITS), PX674606 (LSU), PX677344 (*TEF1*), and PX677345 (*RPB1*), respectively. Sequence identity searches against the NCBI GenBank database using BLAST revealed that the ITS sequence of BCC 9612 shared 99.20% identity with *Pleurocordyceps aurantiaca* (voucher MFLU 17-1582, accession no. MG136920). The LSU, *TEF1*, and *RPB1* genes showed 99.66%, 99.71%, and 99.20% identity with *Polycephalomyces* sp. GIMCC 3.570 (JX006098), *Pleurocordyceps ophiocordycipititicola* (OQ186388), and *Polycephalomyces* sp. GIMCC 3.570 (OQ459755), respectively. To further confirm taxonomic placement, a phylogenetic analysis based on a combined dataset of 53 taxa using

multi-locus sequence data was conducted. The resulting phylogenetic tree (Fig. S91) placed strain BCC 9612 in the same clade as *Pleurocordyceps ophiocordycipiticola* MFLUCC 22-0265, as proposed by Wei *et al.*,[10] thereby supporting the identification of strain BCC 9612 as *P. ophiocordycipiticola* (Ophiocordycipitaceae, Hypocreales, Hypocreomycetidae, Sordariomycetes, Pezizomycotina, Ascomycota, fungi).

Culture conditions

The fungus TBRC-BCC 9612 was initially cultivated on potato dextrose agar (PDA). Agar cultures were cut into small cubes (1 × 1 cm) and used to inoculate four 250 mL Erlenmeyer flasks, each containing 25 mL of potato dextrose broth (PDB; composed of 4.0 g per L potato starch and 20.0 g per L dextrose in distilled water). The seed cultures were incubated at 25 °C for 7 days on a rotary shaker at 200 rpm. Subsequently, each primary culture was transferred into 1 L Erlenmeyer flasks containing 250 mL of the same medium and incubated under identical conditions for 7 additional days. For large-scale fermentation, 25 mL aliquots of the secondary culture were then used to inoculate forty 1 L Erlenmeyer flasks, each containing 250 mL of YES medium (composition: yeast extract, 20.0 g; sucrose, 150.0 g; adjusted to 1000 mL with distilled water; pH 7.0). The fermentation was carried out under static conditions at 25 °C for 35 days.

Extraction and isolation

The fermentation culture was filtered to separate the mycelial biomass from the culture broth. The broth was extracted with ethyl acetate (EtOAc) three times (3 × 10 L), and the combined organic layers were concentrated under reduced pressure to yield a dark brown gum (extract A, 2.77 g). The separated mycelia were sequentially macerated in methanol (MeOH, 1 L) for three days, followed by dichloromethane (CH_2Cl_2, 1 L) for another three days. The combined MeOH and CH_2Cl_2 extracts were concentrated under reduced pressure to afford a crude residue, which was then partitioned between water (800 mL) and *n*-hexane (3 × 800 mL), followed by extraction with EtOAc (3 × 800 mL). The combined *n*-hexane and EtOAc layers were separately concentrated under reduced pressure to yield crude brown gummy extracts: 6.12 g from the *n*-hexane fraction (extract B) and 0.52 g from the EtOAc fraction (extract C).

Extract A was triturated with MeOH, and the resulting suspension was filtered to afford a brown solid (0.59 g). This solid was subjected to purification by preparative HPLC using a linear gradient elution of MeCN–H_2O containing 0.01% TFA (0–15% over 50 min), yielding compound cordytropolone (64.3 mg). The remaining residue was fractionated by Sephadex LH-20 chromatography using MeOH as the eluent to furnish six fractions (A1–A6). Fraction A3 was further chromatographed on a Sephadex LH-20 column with MeOH to afford five subfractions (A3.1–A3.5). Compound **6** (16.8 mg) was obtained from subfraction A3.5. Subfraction A3.3 was subsequently subjected to preparative HPLC (MeCN–H_2O, 10–100% linear gradient over 40 min), yielding compounds **1** (7.9 mg), **2** (21.4 mg), **7** (4.8 mg), **8** (6.5 mg), akanthomycin (12.5 mg), and cordypyridones A (2.5 mg), and C (8.3 mg). Purification of subfraction A3.4 by preparative HPLC (MeCN–H_2O, 10–100% over 45 min) obtained cordypyridones A (7.8 mg) and B (6.4 mg). Fraction A4 was also purified by preparative HPLC (MeCN–H_2O, 10–100% over 40 min) to afford compounds **3** (8.4 mg), **4** (9.8 mg), **5** (5.4 mg), **6** (36.5 mg), and cordypyridones A (17.1 mg) and B (16.6 mg). Further purification of fraction A5 using preparative HPLC (MeCN–H_2O, 5–70% over 40 min) yielded compound **6** (20.3 mg) and 3-methylorcinaldehyde (4.2 mg). Finally, purification of fraction A6 by preparative HPLC (MeCN–H_2O with 0.05% TFA, 5–70% over 55 min) furnished stipitalide (0.5 mg), cordytropolone (1.0 mg), indole-2-carboxylic acid (0.9 mg), and 3-methylorcinaldehyde (0.5 mg).

Extract B was subjected to chromatography on a Sephadex LH-20 column eluted with MeOH, affording eleven fractions (B1–B11). Compound **9** (1.7 mg), 3-methylorcinaldehyde (26.9 mg), and stipitalide (0.9 mg) were obtained from fractions B7, B10, and B11, respectively. Fractions B5 and B6 were triturated with MeOH and filtered to yield ergosterol (243.9 mg) as a pale-yellow solid. The filtrate from B5 was further purified by Sephadex LH-20 column chromatography (100% MeOH), followed by preparative HPLC (linear gradient elution with MeCN–H_2O, 30–100%) to afford *trans–trans*-farnesol (8.7 mg) and cordypyridones A (3.9 mg), B (5.0 mg) and C (9.6 mg). The residue from fraction B6 was purified by preparative HPLC (MeCN–H_2O, 30–100% over 40 min), yielding cordypyridones A (52.7 mg), B (46.7 mg) and C (5.1 mg).

In a separate procedure, extract C was directly subjected to preparative HPLC, which furnished stipitalide (48.7 mg), cordytropolone (25.5 mg), 4-hydroxy-3,6-dimethyl-2*H*-pyran-2-one (2.9 mg), 3-methylorcinaldehyde (11.7 mg), and cordypyridone B (7.3 mg).

Dihydroergosine (1). Pale-yellow solid; $[\alpha]_D^{27}$ +9.73 (*c* 0.10, $CHCl_3$); UV (MeOH) λ_{max} (log ε) 202 (5.44), 223 (5.38), 279 (4.73) nm; CD (MeOH) $\Delta\varepsilon$ (nm) −13.71 (214), +1.09 (239), −0.33 (265); IR (ATR) ν_{max} 3282, 2957, 2927, 1719, 1638, 1556, 1446, 1364, 1216, 1142, 1037 cm^{-1}; ^1H and ^{13}C NMR data, see Table 1; HRMS (ESITOF) *m*/*z* 550.3025 $[M + H]^+$ (calcd for: $C_{30}H_{39}N_5O_5$ + H, 550.3024).

Dihydroergopleurine (2). Pale-brown solid; $[\alpha]_D^{27}$ −5.32 (*c* 0.11, $CHCl_3$); UV (MeOH) λ_{max} (log ε) 202 (4.48), 223 (4.43), 281 (3.77) nm; CD (MeOH) $\Delta\varepsilon$ (nm) −10.51 (214), +0.89 (239), −0.24 (269); IR (ATR) ν_{max} 3266, 2958, 2927, 1716, 1638, 1555, 1445, 1363, 1217, 1142, 1035 cm^{-1}; ^1H and ^{13}C NMR data, see Table 1; HRMS (ESITOF) *m*/*z* 564.3187 $[M + H]^+$ (calcd for: $C_{31}H_{41}N_5O_5$ + H, 564.3180).

14-Nor-epicoccarine (3). Pale-yellow solid; $[\alpha]_D^{25}$ −116.87 (*c* 0.09, MeOH); UV (MeOH) λ_{max} (log ε) 201 (4.38), 223 (4.06), 280 (4.09) nm; CD (MeOH) $\Delta\varepsilon$ (nm) +1.30 (216), −5.46 (232), −1.09 (276), −2.57 (292); IR (ATR) ν_{max} 3306, 2959, 2924, 1654, 1604, 1516, 1452, 1377, 1354, 1229 cm^{-1}; ^1H and ^{13}C NMR data, see Table 2; HRMS (ESITOF) *m*/*z* 372.2160 $[M + H]^+$ (calcd for: $C_{22}H_{29}NO_4$ + H, 372.2169).

Pleurocordine A (4). Pale-yellow solid; $[\alpha]_D^{25}$ +77.76 (*c* 0.10, MeOH); UV (MeOH) λ_{max} (log ε) 201 (4.14), 223 (3.87), 280 (3.95) nm; CD (MeOH) $\Delta\varepsilon$ (nm) −0.95 (217), +3.79 (232), +0.60 (275), +1.67 (292); IR (ATR) ν_{max} 3306, 2969, 2924, 1654, 1604, 1516, 1452, 1377, 1353, 1230 cm^{-1}; ^1H and ^{13}C NMR data, see

Table 2; HRMS (ESITOF) *m*/*z* 394.1983 $[M + Na]^+$ (calcd for: $C_{22}H_{29}NO_4$ + Na, 394.1989).

Pleurocordine B (5). Pale-yellow solid; $[\alpha]_D^{25}$ +43.03 (*c* 0.12, MeOH); UV (MeOH) λ_{max} (log ε) 201 (4.34), 224 (4.07), 279 (4.06) nm; CD (MeOH) $\Delta\varepsilon$ (nm) −0.63 (213), +0.84 (229), +0.25 (249) +1.50 (288); IR (ATR) ν_{max} 3307, 2959, 2924, 1653, 1604, 1516, 1455, 1377, 1229 cm^{-1}; ^1H and ^{13}C NMR data, see Table 2; HRMS (ESITOF) *m*/*z* 410.1937 $[M + Na]^+$ (calcd for: $C_{22}H_{29}NO_5$ + Na, 410.1938).

Pleurocordine C (6). Yellow solid; $[\alpha]_D^{25}$ −65.89 (*c* 0.10, MeOH); UV (MeOH) λ_{max} (log ε) 201 (4.30), 244 (4.01), 299 (4.21), 330 (4.15), 361 (4.17) nm; IR (ATR) ν_{max} 3296, 2969, 2925, 1690, 1603, 1516, 1451, 1377, 1276, 1228, 1196, 1173 cm^{-1}; ^1H and ^{13}C NMR data, see Table 2; HRMS (ESITOF) *m*/*z* 392.1833 $[M + Na]^+$ (calcd for: $C_{22}H_{27}NO_4$ + Na, 392.1832).

10-Carboxy-6,10-dimethyl-5*E*,9*Z*-undecadien-2-one (7). Pale-yellow oil; UV (CH_3CN) λ_{max} (log ε) 199 (2.35), 217 (3.83) nm; IR (ATR) ν_{max} 3429, 2957, 2927, 1708, 1644, 1417, 1376, 1257, 1168 cm^{-1}; ^1H NMR (500 MHz, acetone-d_6) δ 6.74 (1H, t, J = 7.0 Hz, H-9), 5.16 (1H, t, J = 6.5 Hz, H-5), 2.47 (2H, t, J = 7.4 Hz, H-3), 2.30 (2H, q, J = 7.4 Hz, H-8), 2.22 (2H, q, J = 7.3 Hz, H-4), 2.11 (2H, t, J = 7.4 Hz, H-7), 2.07 (3H, s, H-1), 1.80 (3H, s, H-11), 1.64 (3H, s, H-12); ^{13}C-NMR (125 MHz, acetone-d_6) δ 207.6 (C-2), 169.1 (C-13), 142.5 (C-9), 135.5 (C-6), 128.5 (C-10), 124.9 (C-5), 43.7 (C-3), 38.9 (C-7), 29.7 (C-1), 27.8 (C-8), 23.0 (C-4), 15.9 (C-12), 12.4 (C-11); HRMS (ESITOF) *m*/*z* 247.1306 $[M + Na]^+$ (calcd for: $C_{13}H_{20}O_3$ + Na, 247.1305).

10-Hydroxy-2,6,10-trimethyl-2*Z*,6*Z*,11-dodecatrienoic acid (8). Pale-yellow oil; $[\alpha]_D^{27}$ −12.94 (*c* 0.11, $CHCl_3$); UV (CH_3CN) λ_{max} (log ε) 213 (4.36) nm; IR (ATR) ν_{max} 3401, 2961, 2926, 1688, 1644, 1417, 1376, 1284, 1247, 1172 cm^{-1}; ^1H NMR (500 MHz, acetone-d_6) δ 6.76 (1H, t, J = 7.0 Hz, H-3), 5.93 (1H, dd, J = 10.7, 17.3 Hz, H-11), 5.21 (1H, d, J = 17.3 Hz, Ha-12), 5.19 (1H, t, J = 7.4 Hz, H-7), 4.96 (1H, d, J = 10.7 Hz, Hb-12), 2.31 (2H, q, J = 7.2 Hz, H-4), 2.11 (2H, t, J = 7.4 Hz, H-5), 2.09 (1H, m, Ha-8), 2.03 (1H, m, Hb-8), 1.80 (3H, s, H-13), 1.62 (3H, s, H-14), 1.23 (3H, s, H-15); ^{13}C-NMR (125 MHz, acetone-d_6) δ 169.2 (C-1), 146.9 (C-11), 142.6 (C-3), 134.4 (C-6), 128.4 (C-2), 126.4 (C-7), 111.3 (C-12), 72.8 (C-10), 43.2 (C-9), 38.9 (C-5), 28.3 (C-15), 27.9 (C-4), 23.3 (C-8), 15.9 (C-14), 12.5 (C-13); HRMS (ESITOF) *m*/*z* 275.1620 $[M + Na]^+$ (calcd for: $C_{15}H_{24}O_3$ + Na, 275.1618).

Methyl-5,6-dihydroxy-1,3-dihydroisobenzofuran-4-carboxylate (9). Pale-brown solid; UV (MeOH) λ_{max} (log ε) 219 (3.35), 250 (3.14), 275 (2.88), 333 (2.79) nm; IR (ATR) ν_{max} 3419, 2923, 2853, 1716, 1674, 1461, 1360, 1330, 1297, 1207, 1172, 1050, 1025, 1004 cm^{-1}; ^1H NMR (500 MHz, DMSO-d_6) δ 10.43 (1H, br s, 5-OH), 9.51 (1H, br s, 6-OH), 6.96 (1H, s, H-7), 5.06 (2H, t, J = 2.4 Hz, H-3), 4.88 (2H, t, J = 2.1 Hz, H-1), 3.87 (3H, s, 4-$COOCH_3$); ^{13}C-NMR (125 MHz, DMSO-d_6) δ 169.5 (C=O), 149.0 (C-5), 145.7 (C-6), 129.4 (C-3a, C-7a), 113.0 (C-7), 107.8 (C-4), 74.3 (C-3), 72.4 (C-1), 52.4 (OCH_3); HRMS (ESITOF) *m*/*z* 233.0421 $[M + Na]^+$ (calcd for: $C_{10}H_{10}O_5$ + Na, 233.0420).

Biological assays

Antimalarial activity against *Plasmodium falciparum* K1 was evaluated using the microculture radioisotope technique.[37] Cytotoxic activity was assessed by the resazurin microplate assay (REMA) against cancer cell lines, including MCF-7 (human breast carcinoma, ATCC HTB-22) and NCI-H187 (human small-cell lung carcinoma, ATCC CRL-5804).[38] Cytotoxicity toward non-cancerous cells was evaluated against Vero cells (African green monkey kidney fibroblasts, ATCC CCL-81) using the green fluorescent protein microplate assay (GFPMA).[39]

Anti-phytopathogenic fungal activity was determined using the 5(6)-carboxyfluorescein diacetate (CFDA) fluorometric assay against *Colletotrichum acutatum* (BCC 58146) and *Alternaria brassicicola* (BCC 42724).[40–42] Antibacterial activities against *Bacillus cereus* (ATCC 11778), *Staphylococcus aureus* (ATCC 29213), and *Acinetobacter baumannii* (ATCC 19606) were performed following the standard protocols recommended by the Clinical and Laboratory Standards Institute (CLSI).[43,44]

Conflicts of interest

All authors declare that they have no conflicts of interest.

Data availability

The data supporting this article have been included as part of the supplementary information (SI). Supplementary information: NMR and MS spectra and RAxML tree of *Pleurocordyceps* and related species. See DOI: https://doi.org/10.1039/d5ra09809b.

Acknowledgements

This research was supported by the National Science, Research and Innovation Fund, Thailand Science Research and Innovation (TSRI) (Grant No. FFB690024/0337) through the National Science and Technology Development Agency (P 2551409).

References

1 V. M. Corbu, I. Gheorghe-Barbu, A. Dumbravă, C. O. Vrâncianu and T. E. Șesan, *Microorganisms*, 2023, **11**, 1384.
2 K. Wadhwa, N. Kapoor, H. Kaur, E. A. Abu-Seer, M. Tariq, S. Siddiqui, V. K. Yadav, P. Niazi, P. Kumar and S. Alghamdi, *Mycobiology*, 2024, **52**, 335–387.
3 A. A. Brakhage, *Nat. Rev. Microbiol.*, 2013, **11**, 21–32.
4 N. P. Keller, G. Turner and J. W. Bennett, *Nat. Rev. Microbiol.*, 2005, **3**, 937–947.
5 I. Molnár, D. Gibson and S. Krasnoff, *Nat. Prod. Rep.*, 2010, **27**, 1241–1275.
6 B. Shrestha, W. Zhang, Y.-J. Zhang and X. Liu, *Mycol. Prog.*, 2012, **11**, 599–614.
7 L. Zhang, O. E. Fasoyin, I. Molnár and Y. Xu, *Nat. Prod. Rep.*, 2020, **37**, 1181–1206.
8 S. A. Survase, L. D. Kagliwal, U. S. Annapure and R. S. Singhal, *Biotechnol. Adv.*, 2011, **29**, 418–435.
9 H. S. Tuli, S. S. Sandhu and A. K. Sharma, *Biotechnology*, 2014, **4**, 1–12.

10 D. P. Wei, E. Gentekaki, D. N. Wanasinghe, S. M. Tang and K. D. Hyde, *Mycosphere*, 2022, **13**, 281–351.
11 A. Sangdee, K. Sangdee, P. Seephonkai, P. Jaihan and T. Kanyaphum, *Int. J. Med. Mushrooms*, 2017, **19**, 445–455.
12 P. Somsila, U. Sakee, A. Srifa and W. Kanchanarach, *J. Pure Appl. Microbiol.*, 2018, **12**, 567–576.
13 W. Sonyot, S. Lamlertthon, J. J. Luangsa-Ard, S. Mongkolsamrit, K. Usuwanthim, K. Ingkaninan, N. Waranuch and N. Suphrom, *Antibiotics*, 2020, **9**, 274.
14 M. Gokhale, D. Raj, I. Deshpande and J. Mycol, *Plant Pathol.*, 2020, **50**, 57–66.
15 P. G. Mantle and E. S. Waight, *Nature*, 1968, **218**, 581–582.
16 A. Stoll and A. Hofmann, *Helv. Chim. Acta*, 1943, **26**, 2070–2081.
17 M. Buchta and L. Cvak, in *Medicinal and Aromatic Plants – Industrial Profiles, vol. 6. Ergot: The Genus Claviceps*, ed. V. Kren and L. Cvak, Harwood Academic Publishers, Amsterdam, 1999, pp. 173–201.
18 E. L. Komarova and O. N. Tolkachev, *Pharm. Chem. J.*, 2001, **35**, 504–513.
19 C. L. Schardl, D. G. Panaccione and P. Tudzynski, *The Alkaloids: Chemistry and Biology*, 2006, vol. 63, pp. 45–86.
20 H. V. Kemami Wangun and C. Hertweck, *Org. Biomol. Chem.*, 2007, **5**, 1702–1705.
21 Y. Ujihara, K. Nakayama, T. Sengoku, M. Takahashi and H. Yoda, *Org. Lett.*, 2012, **14**, 5142–5145.
22 Z. Shang, L. Li, B. P. Espósito, A. A. Salim, Z. G. Khalil, M. Quezada, P. V. Bernhardt and R. J. Capon, *Org. Biomol. Chem.*, 2015, **13**, 7795–7802.
23 C. A. Lindsay, C. Y. Tan, D. Krishnan, D. Uchenik, G. D. Anaya Eugenio, E. D. Salinas, E. J. Carcache de Blanco, A. D. Kinghorn and H. L. Rakotondraibe, *Phytochem. Lett.*, 2024, **63**, 79–86.
24 K. L. Eley, L. M. Halo, Z. Song, H. Powles, R. J. Cox, A. M. Bailey, C. M. Lazarus and T. J. Simpson, *ChemBioChem*, 2007, **8**, 289–297.
25 M. Ohashi, C. S. Jamieson, Y. Cai, D. Tan, D. Kanayama, M.-C. Tang, S. M. Anthony, J. V. Chari, J. S. Barber, E. Picazo, T. B. Kakule, S. Cao, N. K. Garg, J. Zhou, K. N. Houk and Y. Tang, *Nature*, 2020, **586**, 64–69.
26 C. S. Jamieson, M. Ohashi, K. N. Houk and Y. Tang, *J. Am. Chem. Soc.*, 2022, **144**, 5280–5283.
27 A. Müller, W. R. Abraham and K. Kieslich, *Bull. Soc. Chim. Belg.*, 1994, **103**, 405–423.
28 H. A. Arfmann, W.-R. Abraham and K. Kieslich, *Biocatal. Biotransform.*, 1988, **2**, 59–67.
29 M. M. Wagenaar, D. M. Gibson and J. Clardy, *Org. Lett.*, 2002, **4**, 671–673.
30 M. Isaka, M. Tanticharoen, P. Kongsaeree and Y. Thebtaranonth, *J. Org. Chem.*, 2001, **66**, 4803–4808.
31 P. Seephonkai, M. Isaka, P. Kittakoop, S. Trakulnaleamsai, R. Rattanajak, M. Tanticharoen and Y. Thebtaranonth, *J. Antibiot.*, 2001, **54**, 751–752.
32 M. Holík and I. Kuhr, *J. Chem. Soc., Chem. Commun.*, 1973, 65–66.
33 A. Hirota, N. Aya, T. Yukiko, H. Hiroshi and N. Abe, *Biosci., Biotechnol., Biochem.*, 1999, **63**, 418–420.
34 T. Bruun, *Acta Chem. Scand.*, 1971, **25**, 2837–2851.
35 R. B. Bates, D. M. Gale and B. J. Gruner, *J. Org. Chem.*, 1963, **28**, 1086–1089.
36 S. Mongkolsamrit, A. Khonsanit, D. Thanakitpipattana, K. Tasanathai, W. Noisripoom, S. Lamlertthon, W. Himaman, J. Houbraken, R. A. Samson and J. Luangsa-ard, *Stud. Mycol.*, 2020, **95**, 171–251.
37 R. E. Desjardins, C. J. Canfield, J. D. Haynes and J. D. Chulay, *Antimicrob. Agents Chemother.*, 1979, **16**, 710–718.
38 J. O'Brien, I. Wilson, T. Orton and F. Pongnan, *Eur. J. Biochem.*, 2000, **267**, 5421–5426.
39 L. Hunt, M. Jordan, M. De Jesus and F. M. Wurm, *Biotechnol. Bioeng.*, 1999, **65**, 201–205.
40 E. A. Aremu, T. Furumai, Y. Igarashi, Y. Sato, H. Akamatsu, M. Kodama, H. Otani and J. Gen, *Plant Pathol.*, 2003, **69**, 211–217.
41 J. Guarro, I. Pujol, C. Aguilar, C. Llop and J. Fernández-Ballart, *J. Antimicrob. Chemother.*, 1998, **42**, 385–387.
42 R. P. Haugland, in *Handbook of Fluorescent Probes and Research Products*, ed. J. Gregory, Molecular Probes, Inc., Oregon, USA, 2022, p. 966.
43 CLSI, *Methods for Dilution Antimicrobial Susceptibility Tests for Bacteria that Grow Aerobically; Approved Standard*, Clinical and Laboratory Standards Institute, 7th edn, CLSI document M7-A7, 2006.
44 CLSI, *Performance Standards for Antimicrobial Susceptibility Testing; 16th Informational Supplement*, Clinical and Laboratory Standards Institute, CLSI document M100-S16, 2006.